Behavior of Ultra-High-Performance Concrete with Hybrid Synthetic Fiber Waste Exposed to Elevated Temperatures

Bassam, Tayeh; Hadzima-Nyarko, Marijana; Riad Riad, Magdy Youssef; Abdel Hafez, Radwa Defalla

buildings

MDPI

Article

Behavior of Ultra-High-Performance Concrete with Hybrid Synthetic Fiber Waste Exposed to Elevated Temperatures

Bassam Tayeh [1,*], Marijana Hadzima-Nyarko [2,3], Magdy Youssef Riad Riad [4] and Radwa Defalla Abdel Hafez [5]

[1] Civil Engineering Department, Faculty of Engineering, Islamic University of Gaza, Gaza Strip P.O. Box 108, Palestine
[2] Faculty of Civil Engineering and Architecture Osijek, Josip Juraj Strossmayer University of Osijek, Vladimira Preloga 3, 31000 Osijek, Croatia
[3] Faculty of Civil Engineering, Transilvania University, 500036 Brașov, Romania
[4] Civil Engineering Department, High Institute of Engineering, Shrouk Academy, El Shorouk 02/82524, Egypt
[5] Civil and Architectural Constructions Department, Faculty of Technology and Education, Sohag University, Arab El Atawla 02/82524, Egypt
* Correspondence: btayeh@iugaza.edu.ps

Abstract: The reinforcement of ultra-high-performance concrete (UHPC) with fibers was investigated in this study. Concrete is the most widely used manmade construction material, and UHPC has remarkable mechanical properties. The mechanical properties of UHPC can be modified by a variety of curing procedures and the amount of cement used. This study aimed to examine the impact of fiber reinforcement, temperature, and exposure time on UHPC. Initially, the temperature for UHPC was changed from 300 °C to 500 °C and the exposure time set to 1 and 2 h. Various combinations of the ultrasonic pulse, thermal conductivity, compressive strength, flexural strength, splitting, modulus of elasticity, and drop hammer impact (impact resistance, impact energy, and ductility index) were investigated after 91 days of steam curing. For steam curing, the temperature was kept at 90 °C for three days. The mechanical characteristics of UHPC were the primary focus of this research. The test results showed that the accelerated curing regime achieved a maximum compressive strength of 102.6 MPa for UHPC specimens without fibers and 124.7 MPa for UHPC specimens with fibers, which represents a 22% increase in compressive strength. When compared to UHPC without fibers, all the qualities of UHPC with fibers were improved, especially when subjected to high temperatures. The incorporation of hybrid synthetic waste fibers was a key aspect in developing new ultra-high-strength concrete features.

Keywords: destructive tests (DTs); nondestructive tests (NDTs); microstructure analysis; strength of ultra-high-performance concrete (UHPC) with fiber reinforcement; elevated temperature; hybrid synthetic waste fibers (HSWFs)

Citation: Tayeh, B.; Hadzima-Nyarko, M.; Riad, M.Y.R.; Hafez, R.D.A. Behavior of Ultra-High-Performance Concrete with Hybrid Synthetic Fiber Waste Exposed to Elevated Temperatures. *Buildings* **2023**, *13*, 129. https://doi.org/10.3390/buildings13010129

Academic Editor: Abdelhafid Khelidj

Received: 27 September 2022
Revised: 9 November 2022
Accepted: 16 November 2022
Published: 4 January 2023

1. Literature Review

Due to its greater strength and durability, ultra-high-performance concrete (UHPC) has been recognized as an intriguing alternative construction material [1]. Its remarkable mechanical characteristics make it a good material for increasing the performance of civil engineering structures [2]. Ultra-high-performance concrete (UHPC) reinforced with fibers [3] is one of the most recent developments in concrete technology. To compensate for the fact that concrete is weak in tension but strong in compression, fibers can be added to the mix to increase strength and structural integrity [4,5]. By using hybrid fibers, it is possible to improve the structural performance of concrete. Hybrid fibers are made by mixing two or more fibers [6,7]. The mechanical properties of fiber concrete, which affect its practical application on construction sites [8], are highly dependent on several factors [9], including the type of cementation materials employed, aggregate size, curing conditions, specimen shape and size, and loading rate [10,11]. Due to its very

high compressive strength (ranging from 150 MPa up to 800 MPa) and very low porosity, UHPC has remarkably low permeability and outstanding durability [12]. Despite its high compressive strength, UHPC demonstrates poor behavior due to brittleness [13]. Radwa Defalla (2019) found that a high percentage of compressive strength could be obtained at the early ages of concrete for all UHPC mixes, which was also attributed to the steam treatment used in the study. The results revealed that all the UHPC mixes had high compressive strength; however, the values varied depending on the components used for these UHPC mixes [14]. Concrete may catch fire in extreme situations. It is widely accepted that high temperatures, as well as the accompanying heating and cooling regimes, cause fundamental physical and chemical changes in concrete, resulting in performance loss [15–18]. Thermal decomposition is more likely in high-strength concrete with a more compact internal structure than in conventional concrete. The fire safety specification set by the construction requirements must be met by the concrete structural elements of buildings [14,18]. The period during which a structural element shows uncertainty regarding its stability, the consistency of the structure, and the temperature transfer is known as the fire resistance [19,20]. Concrete generally has the best fire resistance of any building material [21]. The behavior of concrete elements exposed to high temperatures is influenced by the mechanical, thermophysical, and deformation properties of concrete components, which change dramatically at such temperatures. The degree of hydration, compressive strength, and modulus of elasticity show a linear relationship that decreases monotonically with increasing heating temperature and duration of exposure [22,23]. It has been found that the effects of temperature on the properties of high-strength concrete differ from those for low-strength concrete [24,25]. In addition to mechanical, thermal, and deformation properties, spalling is described as the falling of concrete components from the face of concrete subjected to high temperatures [26,27]. UHPC is more prone to fire-induced spalling than conventional-strength concrete due to its lower water-to-cement ratio and low permeability [28,29]. The current study examined the effectiveness of UHPC at temperatures of 300 °C and 500 °C for exposure durations of 1 and 2 h, using hybrid synthetic waste fibers (HSWFs) as traditional, cheap, and sustainable fibers to enhance its brittle behavior. To achieve this objective, ten UHPC mixtures were designed and cast; the first two mixtures were UHPC control mixtures without and with hybrid synthetic waste fibers. The control UHPC mixture with hybrid synthetic waste fibers (HSWFs) was designed to attain strength equivalent to 102.6 MPa when HSWFs were used at a 1% by volume ratio. This ratio was calculated based on earlier research, since the optimal performance of fibers in improving concrete qualities was found to be approximately that value. To evaluate the hardened characteristics of concrete, tests of the compressive strength after 91 days, splitting, flexural strength, modulus of elasticity, ultrasonic pulse velocity (UPV), thermal conductivity, and impact energy were performed. Finally, microstructural investigations were carried out to confirm and validate previous test results.

This study investigated how elevated temperatures and exposure duration impact the strength of UHPC reinforced with fibers. The use of hybrid synthetic fiber waste can help to reduce cracks in concrete that can cause damage to the concrete structure. Based on the relevant research in the current study, the following conclusions may be drawn:

1. The significance of this work is the investigation of destructive and nondestructive testing of UHPC reinforced with hybrid synthetic waste fibers exposed to elevated temperatures, a topic that has never been thoroughly researched'
2. Hybrid synthetic fiber waste can be utilized in the production of UHPC;
3. It was determined that it is possible to produce UHPC containing hybrid synthetic waste fibers with a compressive strength of 124.7 MPa after 91 days;
4. The effects of hybrid synthetic waste fibers, temperature degree, and exposure time were investigated through nondestructive and destructive tests, and a microstructure analysis was also performed;
5. Further research should be conducted in the UHPC sector with diverse influencing factors to study UHPC behavior extensively.

2. Experimental Program

To fulfill the aims of the current work, a concrete mix with a compressive strength of 102.6 MPa was constructed in the first stage of the experimental program. The details of the mixture's proportions are given in Table 1. To obtain ultra-high strength, these mixtures used limited amounts of cement type CEM I—52.5. In addition, silica fume was added to the cement with a silica content of 20%, a specific gravity of 2.15, and a specific surface area of 20,000 cm^2/gm. Gravel aggregates were used with sizes of 5 mm and 10 mm, and natural sand was used as a fine aggregate. Furthermore, instead of aggregates, locally produced quartz powder (QP) was used as filler in the mixes. A high-performance superplasticizer concrete additive (Viscocrete-5930, which conforms to ASTM C494 Type G and F and BS EN 934 Part 2) was included in the proposed mix to reduce the amount of mixing water. To keep the water/binder material ratio in the UHPC mixes as low as possible, the additive dose was 2% of the cement content in the mix [30]. Different types of hybrid synthetic waste fibers (HSWFs) with different lengths were used in the mixture at 1% by volume to increase the flexural strength of the mixture, as shown in Figure 1 and Table 2. This was the minimum water/binder ratio that ensured reasonable and consistent workability. A particular mixing method must be followed to obtain UHPC. As a result, the concrete mixtures were mechanically mixed as follows:

1. For one minute, fine materials (cement, silica fume, HSWF, and quartz powder) were combined in a pan mixer;
2. Half of the mixing water was poured into the pan mixer and mixed for four more minutes;
3. The required amount of admixture was mixed with the remaining half of the water, and then the last mixture was added;
4. Over the next five minutes, the fine aggregate was gradually added, followed by the coarse aggregate, until the mixture was homogenous.

Table 1. Mix proportions of the UHPC specimens.

HSWFs	Water/Binder Ratio	Admixture (kg/m^3)	Water (L/m^3)	QP (kg/m^3)	Natural Fine Aggregates (kg/m^3)	Natural Coarse Aggregates (kg/m^3)		Silica Fume (kg/m^3)	Cement (kg/m^3)	Mix
						Size 5 mm	Size 10 mm			
0%	0.20	13	156	440	440	294	294	130	650	1
1%	0.20	13	156	440	440	294	294	130	650	2

Figure 1. (**a**) Hybrid synthetic waste fibers; (**b**) enlarged image of hybrid synthetic waste fibers; (**c**) the size of the hybrid synthetic waste fibers.

Table 2. Components and physical and mechanical properties of hybrid synthetic waste fibers (HSWFs).

Type of Fiber	Length (mm)	Diameter (mm)	Tensile Strength (MPa)	Elastic Modulus (GPa)	Specific Gravity
Nylon	18	0.05	967	24	1.15
Polyester	10	0.04	901	21	1.08
Polypropylene	6	0.03	860	17	1.00

The effect of curing conditions on the strength of UHPC has been researched in several studies [31,32]. These studies found that three days of steam curing increases concrete's compressive strength. As a result, 24 h later, just one curing condition was used: steam curing at 90 °C for three days following casting, followed by immersion in water until the test time.

In this investigation, three different forms of fiber were used. To create crack patterns for the UHPC, fibers were added to the concrete mixtures. The fibers were derived from left over garbage. Such waste is dangerous to the environment and can pollute the air when burned. To eliminate the dirt and other impurities on the surface, HSWFs—the fibers used in the concrete casting—first had to be cleansed. Sacks containing waste carpets were delivered to the lab, where they underwent repeated water washings to remove dust. Clean carpets were then spread on sheets and dried.

2.1. Specimen Descriptions

For the mixes presented in Table 1, the mechanical and physical properties, such as the compressive strength, splitting strength, flexural strength, modulus of elasticity, ultrasonic pulse velocity, impact energy, and thermal conductivity, were obtained at elevated temperatures (300 °C for 1 h, 300 °C for 2 h, 500 °C for 1 h, and 500 °C for 2 h) 91 days after the casting date. All concrete specimens of each mix were cast in steel molds with dimensions as follows.

- ❖ Nondestructive testing (physical and thermal properties):
  - The ultrasonic pulse velocity was measured with 150 × 150 × 150 mm cubes in accordance with ASTM C 597 [33];
  - A tile of 300 × 300 × 30 mm was used for the thermal conductivity tests in accordance with the specification ASTM C 518 [34].
- ❖ Destructive testing (mechanical properties):
  - Cubes of 150 × 150 × 150 mm were used for the compressive tests in accordance with the specification BS 1881, part 108 [35];
  - Prisms of 100 × 100 × 500 mm were used for the flexural tests in accordance with the specification ASTM C 78 [36];
  - Cylinders of 150 × 300 mm were used for the splitting tests in accordance with the specification ASTM C 192 [37];
  - Cylinders of 150 × 300 mm were used to test the static modulus of elasticity in accordance with the specification ASTM C469/C469 M-14 [38];
  - A tile of 500 × 500 × 50 mm was used for the drop hammer impact test in accordance with the specifications of ACI Committee 544 [39].

2.2. Elevated Temperature Exposure

The samples were then kept at room temperature for 24 h before being steam cured for three days and, finally, tested in ambient air [40,41]. Each specimen was heated in an electrical furnace. The electrical furnace used in the trials had an average heating rate of 10 °C per minute. Four different temperature settings were used in this study: 300 °C and 500 °C for 1 h and 300 °C and 500 °C for 2 h. Unheated specimens were evaluated at ambient temperature as control specimens for comparison.

2.3. Nondestructive Testing

2.3.1. Measurements of Ultrasonic Pulse Velocity

The ultrasonic pulse velocity (UPV) was used to quantify the damage to and residual compressive strength of UHPC exposed to elevated temperatures in the current study. The UPV was measured according to ASTM C 597 with a commercially available pulse velocity meter with an attached transducer pair just before the compression tests for the heated and unheated cube specimens. Several tests were conducted to establish connections between the UPV values and the residual compressive strength of heated concrete. The principle for the UPV measurement was to send a wave pulse through the concrete specimen and measure the travel time. A transmitting transducer generated the pulse, which was detected by a receiving transducer. The procedure was begun by calculating the time it took for the pulse to travel through the concrete followed by the velocity. Once the velocity had been calculated, the concrete's quality uniformity condition and strength were estimated. It was desired that the concrete surface should be smooth, and grease was utilized between the transducers and the specimen surface. To ensure firm contact between the transducers and the specimen surface, application of pressure was also needed.

2.3.2. Thermal Conductivity of Concrete

The heat conductivity of UHPC reinforced with hybrid synthetic waste fibers was determined according to ASTM C518. As test examples, UHPC specimens with dimensions of 300 × 300 × 30 mm were used. Before measuring the thermal conductivity, the cured specimens were dried in an oven until the mass stopped changing. The thermal conductivity in this study was based on the average for three specimens with an accuracy of 0.001 W/mK.

2.4. Destructive Testing

Mechanical Properties (Compressive Strength, Flexural Strength, Splitting Strength, and Modulus of Elasticity)

All specimens of the analyzed UHPC mixtures were subjected to destructive testing after heating, such as testing of the compressive strength, splitting strength, flexural strength, and static modulus of elasticity. Experiments were carried out. As previously indicated, the average of the results for three identical specimens was obtained for each test and then used in the analysis and discussion of the test results. Finally, in the drop hammer impact test, simple tiles with center one-point loading were utilized. All impact stress values were based on one specimen and were evaluated at the age of 91 days.

3. Microstructure Analysis

Extreme temperatures can cause considerable harm to UHPC. As a result, determining whether a heated concrete structure and its components have unraveled or are still structurally sound is crucial. The microstructural features of numerous control and heated specimens were obtained using a scanning electron microscope (SEM) at high magnification.

4. Results

In this section, the results of nondestructive and destructive tests for unheated (control) and heated specimens of the investigated mixtures after 91 days are presented and discussed. This section also examines the influence of factors such as temperature and exposure time on the properties of concrete.

4.1. Results of Nondestructive Testing

The results of nondestructive tests for unheated (control) and heated specimens of the investigated UHPC mixtures after 91 days are described below.

4.1.1. Ultrasonic Pulse Velocity (UPV)

As previously stated, the ultrasonic pulse velocity (UPV) was measured to assess the damage to and residual compressive strength of UHPC exposed to extreme temperatures.

As demonstrated in Figure 2, the measured UPV values of the control specimens increased as the concrete grade increased. The control samples had UPV values of 4815 and 4922 m/s, respectively, indicating that samples containing hybrid synthetic waste fibers with 1% fiber had greater values than the control samples (without fiber), which agrees with previous work [41]. The UPV values of the heated specimens were found to be lower than those of the control specimens. The values for the samples without fibers exposed to temperatures of 300 °C and 500 °C for 1 h and to the same temperatures for 2 h were 4710, 4650, 4601, and 4408 m/s, respectively [41]. The UHPC samples containing HSW fibers, on the other hand, had values of 4816, 4752, 4705, and 4602 m/s for 300 °C for 1 h, 500 °C for 1 h, 300 °C for 2 h, and 500 °C for 2 h, respectively [42–44]. As a result, it is obvious that UHPC with HSW fibers had greater resistance than UHPC without fibers, which was reflected in the sound waves test and explains the recorded values. There was a direct relationship between the concrete grade and the ultrasound velocity: the greater the compressive resistance was, the higher the velocity of the ultrasonic waves. Furthermore, the temperature and exposure duration had negative effects on the ultrasound velocity (Figure 2).

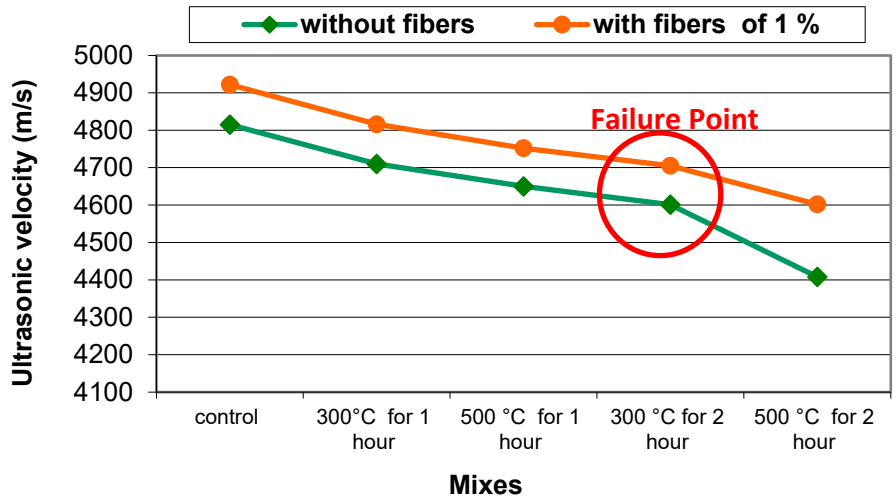

Figure 2. Dependence of the ultrasound velocity on the transmission mode as assessed by the direct method.

4.1.2. Thermal Conductivity

The current study included experimental work to determine the benefits of incorporating hybrid synthetic fiber waste into concrete mixes, aiming to reduce the overall thermal conductivity and heat transfer through construction elements and, thereby, increase thermal insulation and lower electricity consumption for air conditioning equipment. The tests were carried out on concrete specimens with dimensions of 300 × 300 × 30 mm using an electric heater as a heat source. The voltage and current supplied to the heater were controlled via a variable voltage transformer. Four thermocouples were used to deliver heat to the two concrete faces and two heater faces, and they were linked to a temperature recorder to record the heat at the four faces and calculate the temperature difference between the specimens' two faces (T). Temperature measurements were taken at each of the four faces (T1, T2, T3, and T4) over time until a steady state was reached, with T2 and T3 indicating the temperatures of the inner faces and T1 and T2 those of the outer faces. The thermal conductivity coefficient was calculated using the following equation:

$$Q = K * A * \Delta T / t \quad (1)$$

Q (power) = I * V = $(V)^2/R$;
K = the coefficient of thermal conductivity;
A = the area of the two faces of the specimen (0.3 × 0.3 m^2);

ΔT = the difference in heat between the faces of specimens.

$$\Delta T = ((T2 + T3)/2) + ((T1 + T4)/2) \quad (2)$$

T2, T3 = temperatures of internal surfaces of specimens;
T1, T4 = temperatures of external surfaces of specimens;
t = thickness of specimen (0.03 m).

Figure 3 depicts the thermal conductivity of the five mixtures (without and with fibers). As hybrid synthetic fiber waste filled the pores and prevented the occurrence of high thermal conductivity, the conductivity values for the control specimens without and with fibers were 0.25 and 0.20 W/m. K at 20 °C, respectively [45]. The thermal conductivity of UHPC was very low because of the low numbers of pores in this type of concrete. Due to the high resistance of the concrete, the thermal conductivity was reduced for fiber concrete, leading to a greater decrease in the pores, which was reflected in the compressive resistance [46,47]. It was observed that the fibers had a lower thermal conductivity than concrete, which explains the difference in conductivity between the concrete without fibers and the concrete with fibers [47,48]. The thermal conductivity decreased gradually with increasing temperature: the values were 0.21, 0.17, 0.14, and 0.10 W/m. K for 300 °C and 500 °C for 1 h and 300 °C and 500 °C for 2 h, respectively. On the other hand, the values for UHPC with 1% fibers were 0.15, 0.09, 0.05, and 0.02 W/m. K for 300 °C for 1 h, 500 °C for 1 h, 300 °C for 2 h, and 500 °C for 2 h, respectively [49]. As the temperature rose, so did the number of phonon collisions (thermal vibration). This caused a reduction in the mean free path of phonons at high temperatures, reducing conductivity. Thermal conductivity decreased during heating due to an increase in overall porosity and water loss during thermal loading. According to previous research, there is a direct link between concrete's compressive strength and thermal conductivity, which means that, as resistance falls, conductivity increases, and as compressive strength increases, conductivity decreases [50]. As UHPC contains tiny pores, the conductivity values are slightly lower than those of traditional concrete [51].

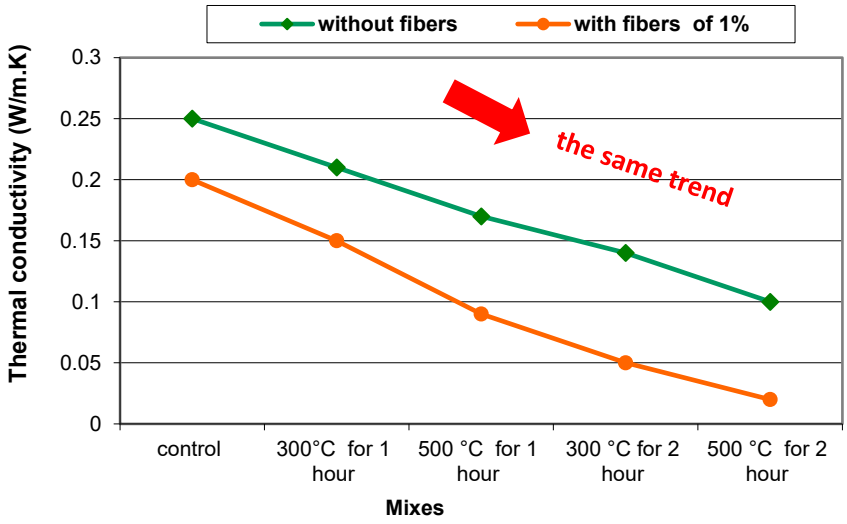

Figure 3. Thermal conductivity of specimens with and without fibers.

4.2. Results of Destructive Testing

4.2.1. Mechanical Properties (Compressive Strength, Flexural Strength, Splitting Strength, and Modulus of Elasticity)

The results of destructive tests for unheated (control) and heated specimens of the investigated UHPC mixtures after 91 days are described below.

Effect of Temperature

As shown in Figure 4, the impacts of high temperatures on the mechanical properties of concrete varied depending on the components. Figure 5 depicts the observed behavior of the concrete specimens as a function of temperature and exposure duration. Due to the thick internal structure of UHPC, vapor discharge at temperatures above 500 °C is troublesome, and the high temperature can cause samples to explode [51–54].

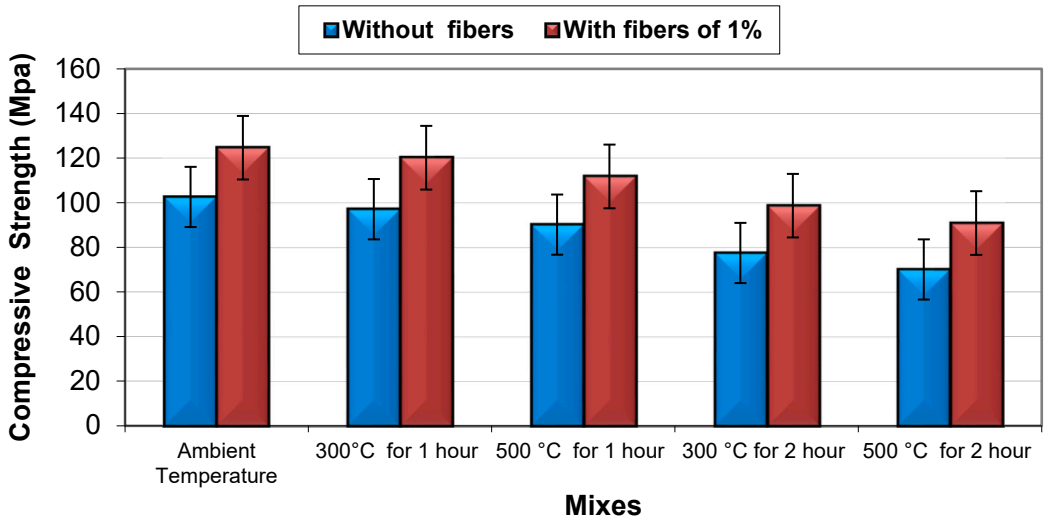

Figure 4. Compressive strengths at various temperatures and exposure times for unheated and heated specimens.

Figure 5. Shapes of specimens after heating.

Heating at 300 °C for 1 h resulted in a 5.36% drop in the compressive strength of the UHPC without fiber but, when 1% fibers were added to the mix, the reduction was 3.61%. After one hour of heating at 500 °C, the compressive strength was reduced by 12.09% and 10.34% compared to unheated specimens for the mixes without and with fibers, respectively. The percentages of the reductions in resistance were substantially larger with exposure for 1 h, with decreases of approximately 24.46% and 20.85% reported for the combinations without and with fibers, respectively. However, after 2 h of exposure to a temperature of 500 °C, the reductions reached 31.68% and 27.11% for mixes with and without fibers, respectively, compared to the unheated specimens.

- Interpretation of results:
  - First, for mixtures without fibers, the phenomenon of decreased resistance with exposure to heat may have been due to the increase in SiO_2 volume induced by heating, which may have canceled out the beneficial effects of reactions, and

these losses in concrete strength may have been connected to the expansion of interior microcracks caused by heating [55,56];

- Second, when mixtures with fibers were subjected to heat, the concrete strength decreased less than the mixtures without fibers because the fibers melted, leaving spaces through which large amounts of heat could escape; therefore, these mixes were less heavily impacted than others. For concrete without fibers, the voids were smaller, leaving less room for large amounts of heat to escape. As a result, internal cracks in the concrete formed to release heat, and these mixes were thus affected more than others, which highlights the importance and usefulness of the presence of fibers in concrete, whether exposed to heat or not. Figure 6 depicts the difference between samples with and without fibers after failure, demonstrating that the presence of fibers preserved the cubes' bonding [57,58].

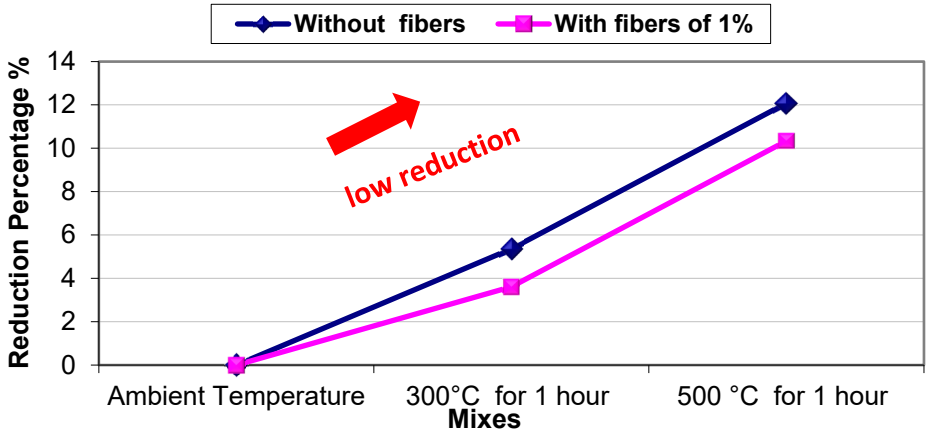

Figure 6. Effect of heating temperature on residual strength at an exposure period of 1 h.

Figures 7–9 show that, when exposed to pressure resistance, the cubes differed in the shape of collapse, and the cubes that did not include fibers collapsed more, while the concrete structures that did contain fibers were retained as much as possible owing to the presence of fibers [55].

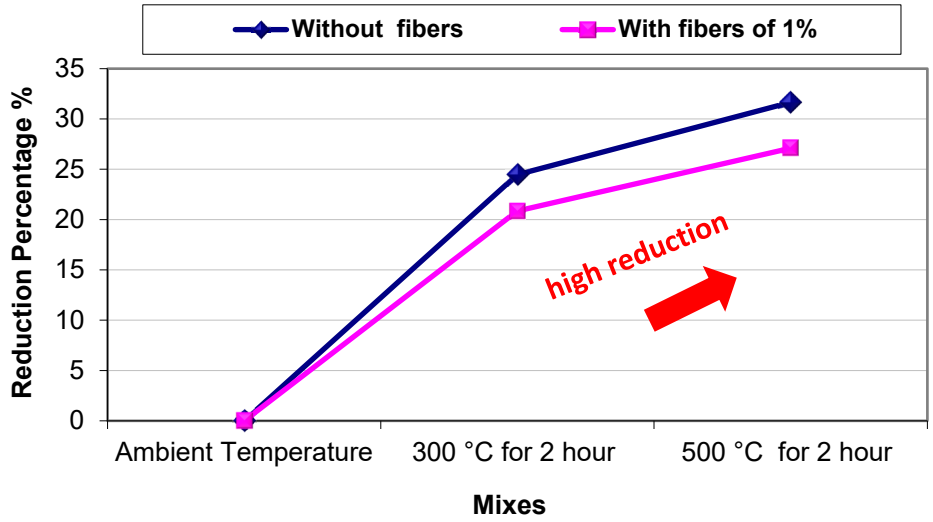

Figure 7. Effect of heating temperature on residual strength at an exposure period of 2 h.

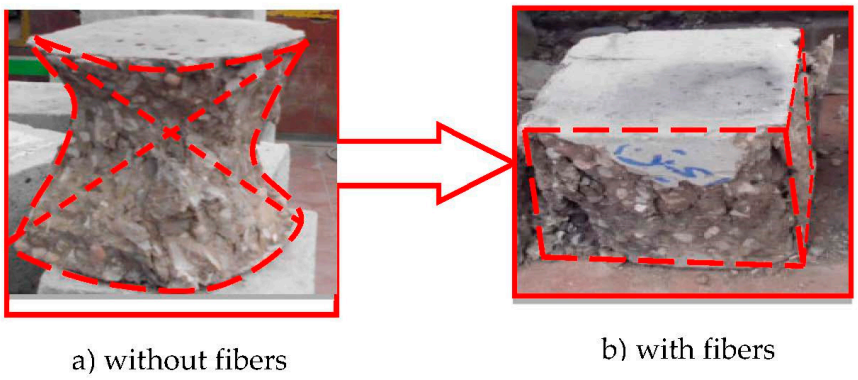

Figure 8. Diagram of failure shape for UHPC cubes: (**a**) without and (**b**) with fibers.

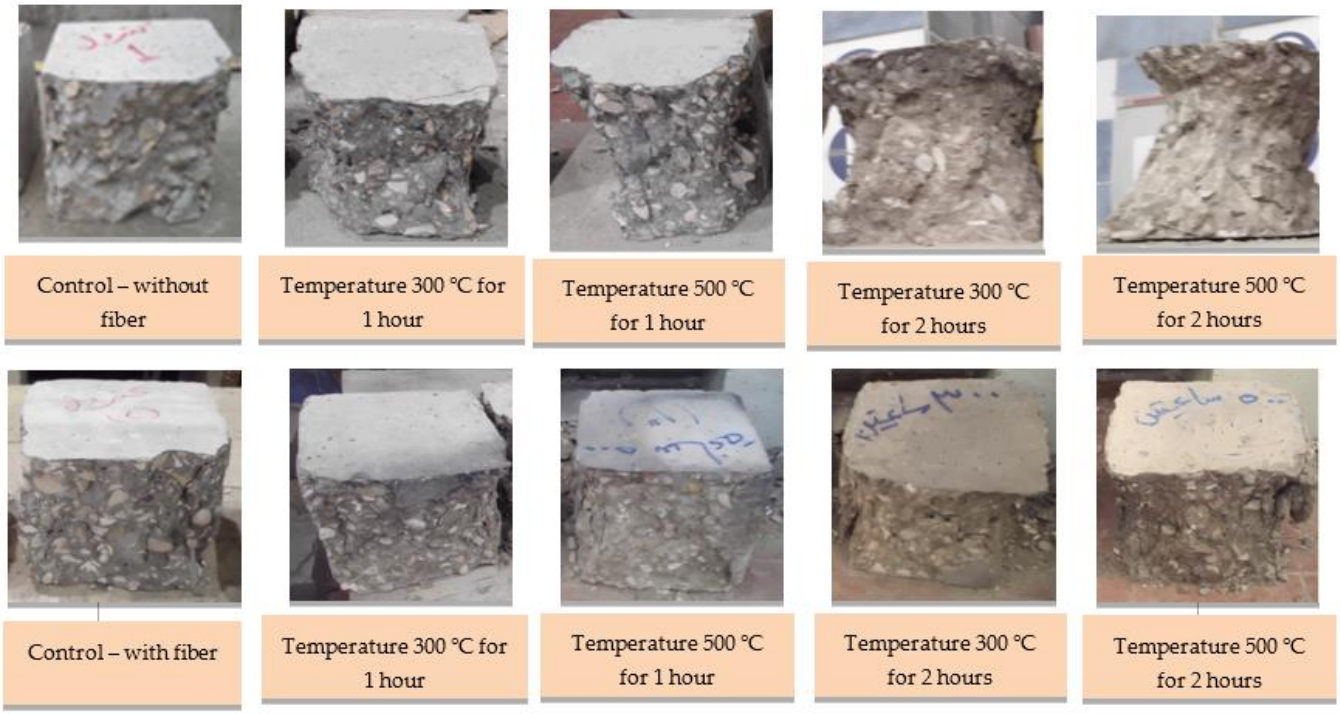

Figure 9. Fracture patterns of UHPC at an age of 91 days.

The values of the other mechanical properties decreased as the temperature rose. The reductions observed in these results were occasionally substantial. For example, the flexural strength, splitting strength, and modulus of elasticity of UHPC specimens without fibers exposed to 300 °C for 1 h were reduced to 7.48%, 5.62%, and 2.42%, respectively, of their control values. On the other hand, the flexural strength, splitting strength, and modulus of elasticity of UHPC specimens with fibers subjected to 300 °C for 1 h were reduced to 7.49%, 5.04%, and 1.76% of their control values, respectively. For lower-temperature blends, large reductions were less noticeable. The flexural strength, splitting strength, and modulus of elasticity of UHPC specimens without fibers exposed to 500 °C for 1 h were reduced to 14.65%, 13.01%, and 6.29% of their unheated values, respectively, and those of UHPC specimens with fibers exposed to the same temperature were reduced to 17.80%, 12.26%, and 5.30%, respectively, of their unheated values [58,59]. This implies that the reductions in mechanical characteristics changed with increasing temperature from 300 °C to 500 °C and the same exposure duration. When the exposure time was prolonged to 2 h at 300 °C, the measured values for UHCP specimens without and with fibers decreased from 27.28%, 26.43%, and 12.83% to 28.30%, 25.18%, and 10.56%, respectively, of their unheated values. Finally, after 2 h of exposure to a temperature of 500 °C degrees, there were

considerable reductions in the values measured for the flexural strength, splitting strength, and modulus of elasticity: 34.53%, 33.98%, and 17.39% of the unheated values, respectively, for UHPC specimens without fibers, and 37.13%, 31.83%, and 14.83% of the unheated values, respectively, for UHPC specimens with fibers [49,60]. It should be noted that the modulus of elasticity for UHPC is slightly lower than that for high-strength and ordinary concrete because the modulus of elasticity decreases with increasing strength. This means that, as the concrete is exposed to longer durations of elevated temperatures, its mechanical properties diminish. Regarding the difference in the rate of damage to mechanical properties between UHPC specimens with and without fibers, this phenomenon can be explained by the fact that, when UHPC specimens with fibers are exposed to elevated temperatures, the fibers fuse, allowing heat to exit through those openings. However, for UHPC specimens without fibers, heat causes what is known as internal cracks. As a result, the damage is greater and the mechanical characteristics are considerably damaged for UHPC without fibers, as shown in Figures 10–13. Figures 10 and 13 show UHPC specimens with fibers where the fracture morphology is fairly cohesive as opposed to UHPC specimens without fibers where the fractures are total cleavages.

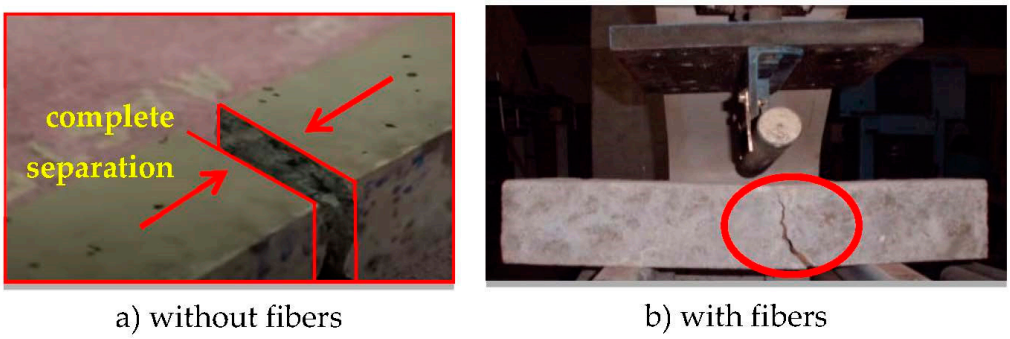

Figure 10. Shape of brims for UHPC specimens with and without fibers after failure.

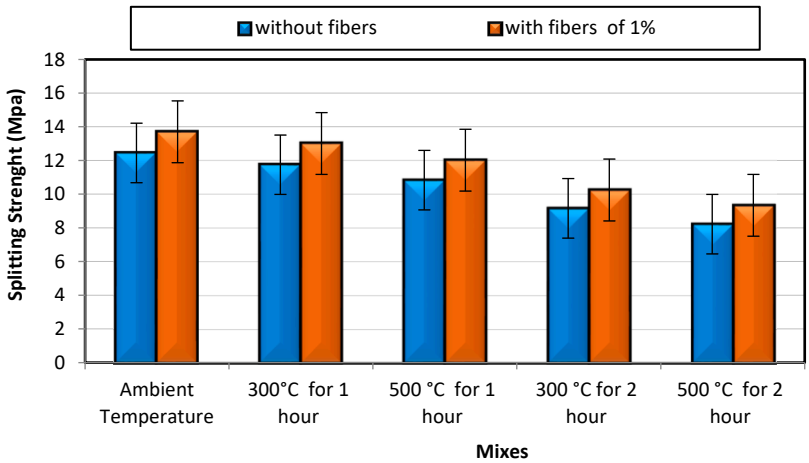

Figure 11. Splitting strength at 91 days for UHPC specimens.

Figure 12. The shapes of cylinders with and without fibers after failure.

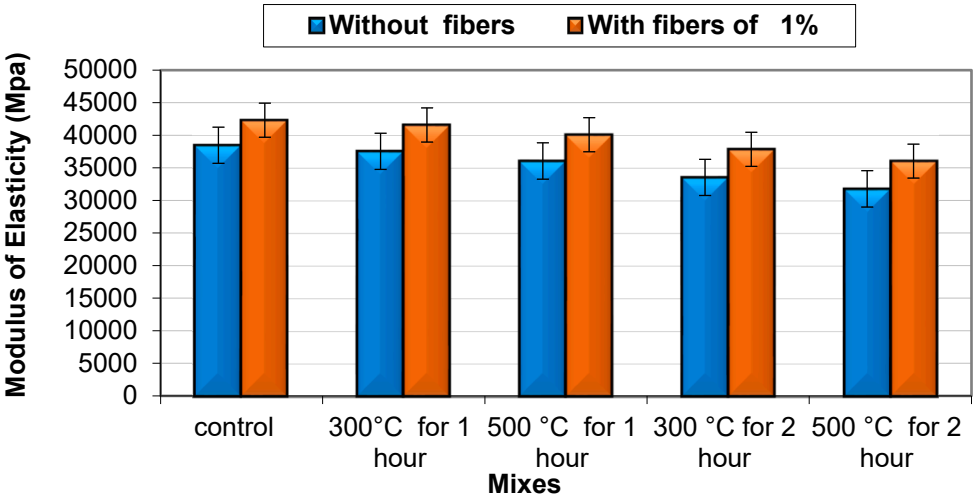

Figure 13. Modulus of elasticity for UHPC specimens.

Effect of Exposure Duration

The investigation included two exposure periods of 1 h and 2 h, as previously noted. Figures 14 and 15 depict the effect of exposure time on the compressive strength of the investigated mixes at temperatures of 300 °C and 500 °C. In general, the compressive strength dropped as the exposure period increased, as shown in the figures. With time, the rate of the reduction in the residual compressive strength increased. For example, after 60 min of exposure to 300 °C, the mix (300 °C for 1 h without fibers) lost 5.36% of its original compressive strength value. After 2 h, the compressive strength loss increased to 24.46%. The rest of the examined blends followed the same pattern. This means that, when concrete is exposed to high temperatures, the compressive strength is reduced. In addition, the other mechanical characteristic values followed the same trend as the compressive strength [51]. For example, after 1 h at the same temperature (300 °C), the residual splitting strength, flexural strength, and modulus of elasticity of one of the mixes (500 °C for 1 h with fibers) were decreased to 7.49.1%, 5.04%, and 1.74%, respectively, of their unheated values. When the exposure time was increased to 2 h, these values were reduced to 28.30%, 25.18%, and 15.27% of their unheated values, respectively.

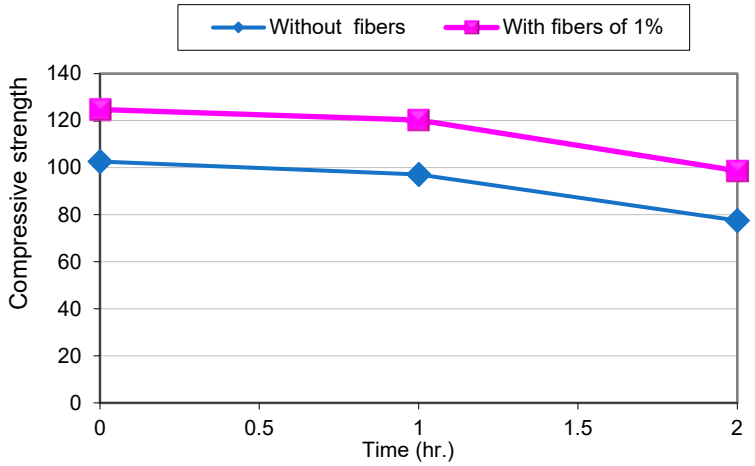

Figure 14. The effect of temperature exposure time at 300 °C on residual compressive strength after 1 h and 2 h.

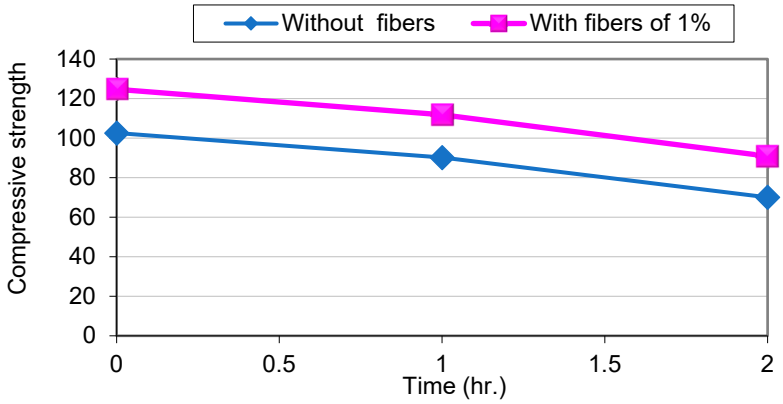

Figure 15. The effect of temperature exposure time at 500 °C on residual compressive strength after 1 and 2 h.

4.2.2. Drop Hammer Impact Test (Impact Resistance)

The drop mass impact test is a simple process that does not require vibration, time history, or displacement measurements. The only criterion for the test is to record the number of impacts until the first crack and failure as shown in Figure 16. A weighted 4.45 kg steel ball was released freely from a height of 0.457 m according to the physical process. Slab concrete was placed on a steel slab disc with four legs to prevent lateral displacement of the specimen during impact. The number of impacts until the first visible crack and failure was recorded. The crack began on the top surface of the cylindrical specimen and continued to the bottom surface, indicating failure. The first crack strength was the number of blows required to cause the first crack on the specimen. The number of blows required to cause large cracks or failure was assessed as the number of impacts required to induce major cracks or failure. The first crack and failure were observed visually, and the total impact energy was calculated using Equation (3):

$$\text{Impact energy (N.m)} = n\ m\ g\ h \quad (3)$$

where:

n—numbers of impacts until the first crack and failure;
m—steel ball mass;
h—the height of the free fall;
g—gravitational acceleration (N/kg).

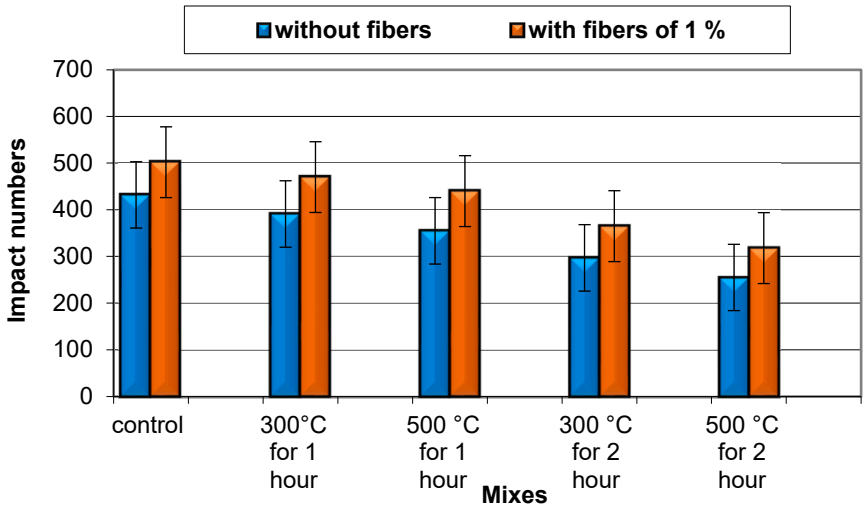

Figure 16. Numbers of impacts needed to create the first crack for UHPC specimens with and without fibers.

The impact ductility index (IDI), which was calculated as the ratio of the failure and first crack impact energy using Equation (4), is an excellent indication of the ductility of concrete exposed to impact loads:

$$\text{Impact ductility index (IDI)} = \text{Failure impact energy}/\text{First crack impact energy} \quad (4)$$

The impact test was undertaken by evaluating four factors: the number of impacts required to produce a fracture, the number of blows required to produce a failure, the impact energy, and the ductility index. Figures 16 and 17 show the experimental results for the impact resistance test in terms of the number of blows and the energy absorption at the reference temperatures. The results demonstrate that adding hybrid synthetic fiber waste to UHPC significantly improved impact resistance and energy absorption. When UHPC specimens with fibers were compared to those without fibers, the number of blows increased by 14% for the first crack and by 16.7% for failure. When subjected to high temperatures, the number of blows decreased. For example, for the number of blows for the first crack, the percentages for UHPC specimens without fibers decreased by 9.50%, 17.82%, 31.25%, and 40.97% compared to the control for 300 °C at 1 h, 500 °C at 1 h, 300 °C at 2 h, and 500 °C at 2 h, but those for UHPC specimens with fibers decreased by 6.37%, 12.35%, 27.29%, and 36.65% compared to the control for 300 °C at 1 h, 500 °C at 1 h, 300 °C at 2 h, and 500 °C at 2 h. Second, the blows to failure for the UHPC specimens without fibers decreased by 5.68%, 12.27%, 23.86%, and 33.41% compared to the control, while the blows to failure for the UHPC specimens with fibers decreased by 3.41%, 7.58%, 19.9%, and 28.60% compared to the control for 300 °C at 1 h, 500 °C at 1 h, 300 °C at 2 h, and 500 °C at 2 h specimens. According to these findings, there is a similarity in behavior between mechanical properties and impact resistance at elevated temperatures, implying that the UHPC with fibers can bear more than UHPC without fibers, with the reduction recorded as having the greatest value being that for the UHPC without fibers, proving the sample's superior behavior in terms of compressive strength. After the first crack formed during the impact test, UHPC specimens lacking fibers exhibited brittle failure. Figures 18 and 19 show that the outcomes of this study are consistent with past studies that found that, depending on the addition ratio, impact energy could increase by 1.22 times for UHPC with fibers and that the impact energy was lowered as temperature and exposure time increased.

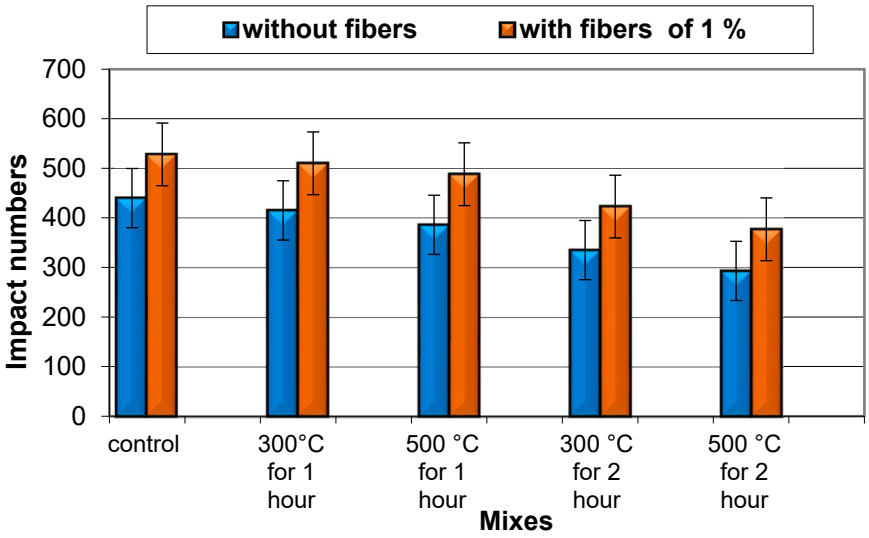

Figure 17. Numbers of impacts to failure for UHPC specimens with and without fibers.

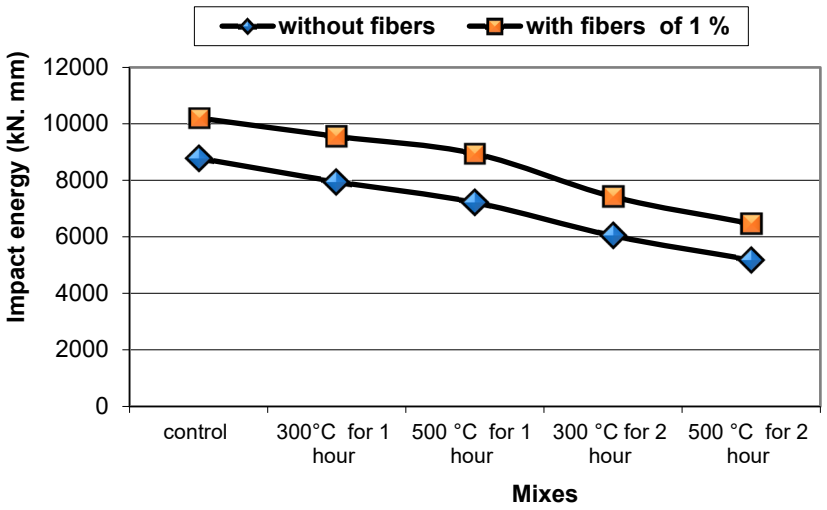

Figure 18. First crack impact energies for UHPC specimens with and without fibers.

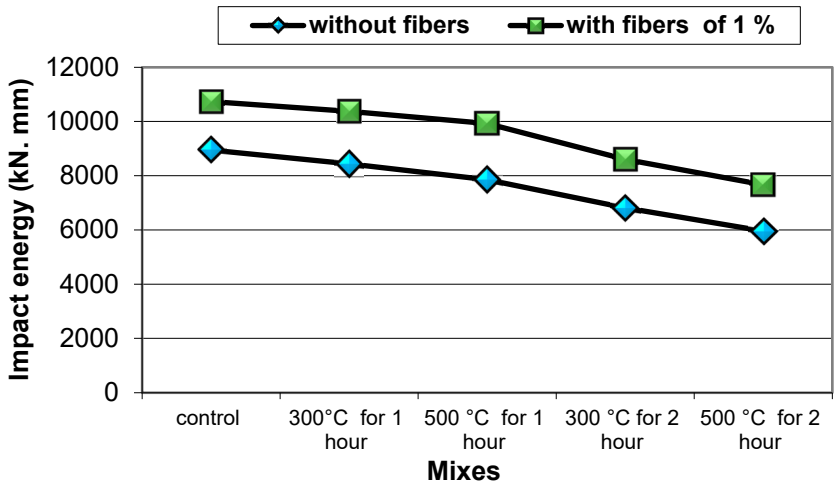

Figure 19. Failure impact energies for UHPC specimens with and without fibers.

Furthermore, due to their low tensile strength, UHPC specimens without fibers had low impact energy [61,62]. Small cracks were visible in the UHPC specimens with fibers

before failure, and the specimens did not split into parts at the maximum load, unlike the specimens without fibers, which failed without warning cracks. This result reveals that hybrid synthetic fiber waste can help in inhibiting the spread of significant fractures. Due to the significant deformation of the fibers, as they were tugged without breaking, more energy was absorbed or lost. The material's impact energy decreased faster than its compressive and tensile strength after being exposed to temperatures of 300 °C and 500 °C. This was due to the increased severity, width, and extension of cracks at high temperatures, resulting in a significant reduction in the ability of fiber concrete to sustain dynamic loads. When fibers were used in concrete, however, the impact energy was increased because the fibers helped in bridging cracks and preventing the specimens from failing suddenly [63]. UHPC resistance to repeated loads could be increased due to the fibers' improved ability to absorb energy, as well as stop and slow down fracture formation at an early stage of loading. Furthermore, repeated impact loads (drop weight) may increase bonding strains for both cement paste and fibers [62]. As demonstrated in Figure 20, UHPC specimens with fibers had a significantly higher ductility index than nonfiber specimens, which had a negligible ductility index. With the increase in the temperature, the ductility also increased, but the highest value was recorded for fiber concrete [64].

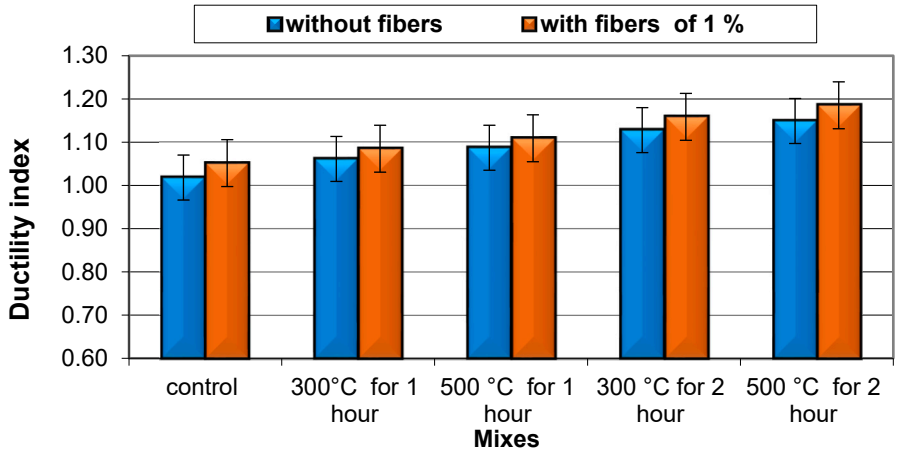

Figure 20. Ductility indexes with and without fiber concrete.

5. Microstructure Analysis

The microstructure analysis included evaluation of the control mix, UHPC specimens without fibers exposed at 500 °C for 2 h, and UHPC specimens with fibers at exposed 500 °C for 2 h. The microstructure had researched due to the specimens' unique mechanical properties.

Scanning Electron Microscopy (SEM)

An electron microscope was used to analyze the microstructure of ultra-high-performance concrete, and a scanning electron microscope (SEM) was used to assess the compositions of samples with and without fiber. Figure 21a clearly shows that the concrete was devoid of fractures and imperfections, which was reflected in the concrete's strength. On the other hand, it was discovered that the UHPC with fibers had greater strength due to the fibers being randomly dispersed in the concrete mixture, which explains why the UHPC with fibers had higher resistance than the other mixes [65,66] (Figure 21b). However, when exposed to high temperatures of up to 500 °C for two hours, the UHPC without fibers was affected more severely than the other mixes [67,68]. When the UHPC with fibers was exposed to high temperatures, the fibers melted, and the heat escaped through the voids, so the heat had little effect on the concrete, which was substantially reflected in its mechanical qualities. As a result, we inferred that, when exposed to elevated temperatures, UHPC with fibers was affected at a lower rate than the other concrete mixes [20,68–70].

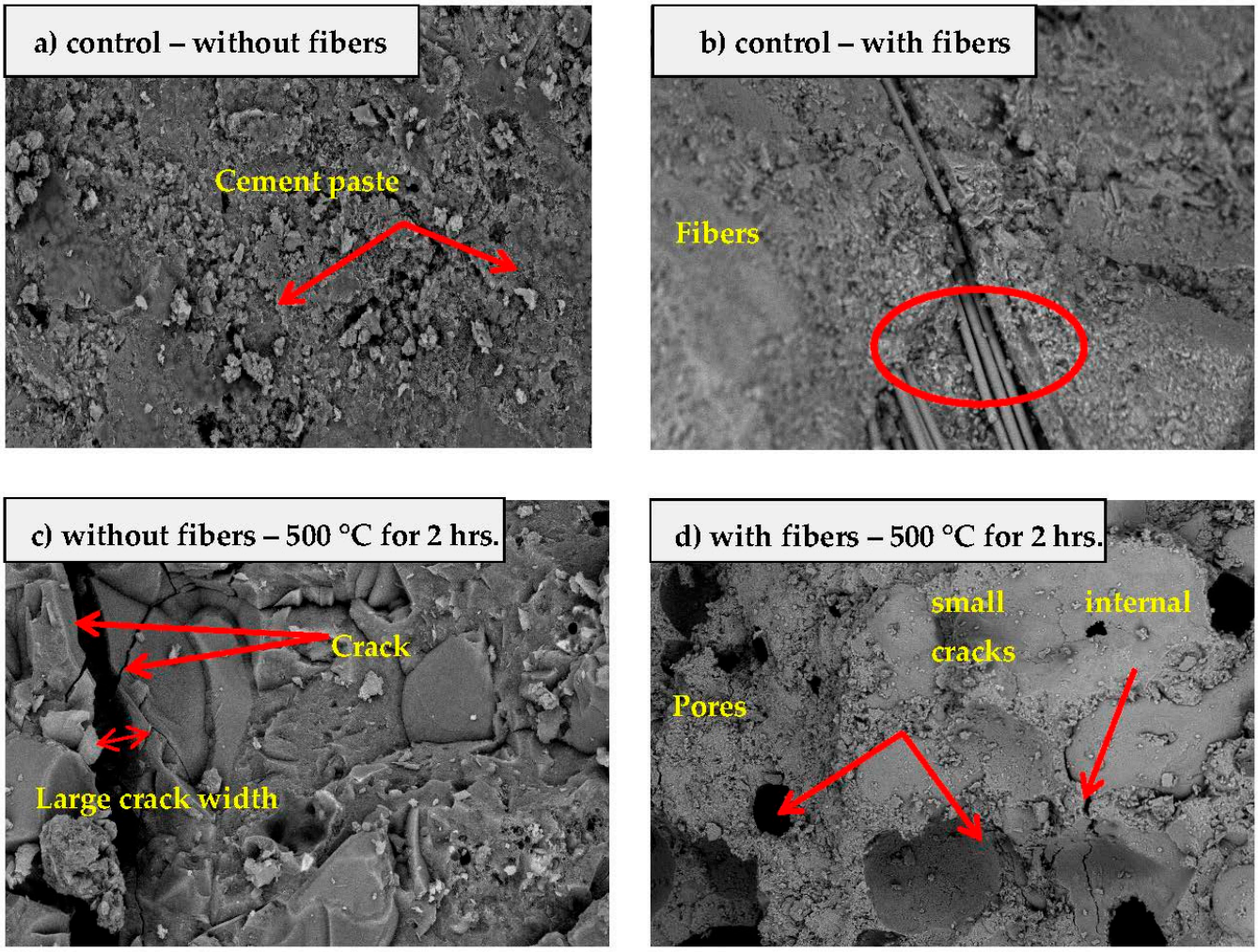

Figure 21. SEM micrographs for: (**a**) control—without fibers, (**b**) control—with fibers, (**c**) specimen without fibers—500 °C for 2 h, and (**d**) specimen with fibers—500 °C for 2 h.

6. Conclusions

The aim of this research was to highlight the incorporation of hybrid synthetic fiber waste as a key aspect in developing a new UHPC. Based on the test results, the following conclusions were reached:

1. There was a direct relationship between concrete grade and ultrasonic velocity: the greater the value of the pressure resistance, the higher the velocity of ultrasonic waves. Furthermore, the temperature and exposure duration had negative effects on the ultrasound values;
2. At high temperatures, the thermal conductivity of UHPC containing hybrid synthetic fiber waste was lower than that of the control group. The heat conductivity reached its maximum after two hours at 500 °C;
3. The decrease in strength of the UHPC with HSW fibers was smaller than that of the UHPC without fibers; this was due to the fibers melting when exposed to heat, leaving spaces through which large amounts of heat could escape and, thus, rendering this concrete mix less affected than the others;
4. The change in the rate of the damage to mechanical properties for the UHPC with and without HSW fibers can be explained by the fact that, when specimens with HSW fibers were exposed to elevated temperatures, the fibers fused, allowing heat to exit via those pores. On the other hand, internal cracks appeared in UHPC specimens

without fibers when heated. As a result, the damage was greater, and the mechanical properties of the UHPC without fibers were considerably impacted;

5. There was a similarity in the behavior relating to the mechanical properties and the impact resistance at elevated temperatures, implying that UHPC with HSW fibers could bear more than UHPC without HSW fibers. The reduction for the UHPC without HSW fibers exhibited the greatest value, highlighting the sample's compressive strength behavior;
6. Small cracks were visible in the UHPC specimens with HSW fibers before failure, and the specimens did not split into pieces at the ultimate load, as was the case with the UHPC specimens without HSW fibers, which collapsed without warning cracks;
7. The enhanced ability of fibers to absorb energy and stop and slow fracture formation at an early stage of loading increased UHPC resistance to repeated loads. Furthermore, the repetition of impact loads increased the strains on the cement paste and the fiber bonding;
8. The behavior of the microstructure revealed that the UHPC without HSW fibers developed huge cracks, but the UHPC with HSW fibers did not develop cracks but rather pores through which large amounts of heat escaped, and these were generated through fiber fusion. As a result, the UHPC without HSW fibers exhibited greater damage than the UHPC with HSW fibers.

Author Contributions: Conceptualization, B.T. and R.D.A.H.; Methodology, B.T. and R.D.A.H.; Investigation, R.D.A.H.; Resources, M.Y.R.R.; Writing—original draft, B.T., M.H.-N. and R.D.A.H.; Writing—review & editing, B.T.; Visualization, B.T.; Funding acquisition, M.Y.R.R. All authors have read and agreed to the published version of the manuscript.

Funding: This research received no external funding.

Data Availability Statement: Not applicable.

Conflicts of Interest: The authors declare no conflict of interest.

References

1. Habel, K.; Viviani, M.; Denarié, E.; Brühwiler, E. Development of the mechanical properties of an Ultra-High Performance Fiber Reinforced Concrete (UHPFRC). *Cem. Concr. Res.* **2006**, *36*, 1362–1370. [CrossRef]
2. Mao, L.; Barnett, S. Investigation of toughness of ultrahigh performance fibre reinforced concrete (UHPFRC) beam under impact loading. *Int. J. Impact Eng.* **2017**, *99*, 26–38. [CrossRef]
3. Yoo, D.-Y.; Shin, H.-O.; Yang, J.-M.; Yoon, Y.-S. Material and bond properties of ultrahigh performance fiber reinforced concrete with micro steel fibers. *Compos. Part B Eng.* **2014**, *58*, 122–133. [CrossRef]
4. Zhang, L.; Hu, Z.; Huang, J.; Chen, Z.; Li, X.; Feng, Z.; Yang, H.; Huang, S.; Luo, R. Experimental and DFT studies of flower-like Ni-doped Mo2C on carbon fiber paper: A highly efficient and robust HER electrocatalyst modulated by $Ni(NO_3)_2$ concentration. *J. Adv. Ceram.* **2022**, *11*, 1294–1306. [CrossRef]
5. Ning, F.; He, G.; Sheng, C.; He, H.; Wang, J.; Zhou, R.; Ning, X. Yarn on yarn abrasion performance of high modulus polyethylene fiber improved by graphene/polyurethane composites coating. *J. Eng. Fibers Fabr.* **2021**, *16*, 1558925020983563. [CrossRef]
6. Huang, H.; Huang, M.; Zhang, W.; Pospisil, S.; Wu, T. Experimental Investigation on Rehabilitation of Corroded RC Columns with BSP and HPFL under Combined Loadings. *Eng. Struct.* **2020**, *146*, 04020157. [CrossRef]
7. Zhang, W.; Huang, Y. Three-dimensional numerical investigation of mixed-mode debonding of FRP-concrete interface using a cohesive zone model. *Constr. Build. Mater.* **2022**, *350*, 128818. [CrossRef]
8. Huang, H.; Guo, M.; Zhang, W.; Huang, M. Seismic Behavior of Strengthened RC Columns under Combined Loadings. *J. Bridg. Eng.* **2022**, *27*, 05022005. [CrossRef]
9. Hu, Z.; Shi, T.; Cen, M.; Wang, J.; Zhao, X.; Zeng, C.; Zhou, Y.; Fan, Y.; Liu, Y.; Zhao, Z. Research progress on lunar and Martian concrete. *Constr. Build. Mater.* **2022**, *343*, 128117. [CrossRef]
10. Yuan, J.; Lei, D.; Shan, Y.; Tong, H.; Fang, X.; Zhao, J. Direct Shear Creep Characteristics of Sand Treated with Microbial-Induced Calcite Precipitation. *Int. J. Civ. Eng.* **2022**, *20*, 763–777. [CrossRef]
11. Wu, Z.; Xu, J.; Li, Y.; Wang, S. Disturbed State Concept–Based Model for the Uniaxial Strain-Softening Behavior of Fiber-Reinforced Soil. *Int. J. Geomech.* **2022**, *22*, 04022092. [CrossRef]
12. Villar-Cociña, E.; Frías, M.; Savastano, H.; Rodier, L.; de Rojas, M.S.; del Bosque, I.S.; Medina, C. Quantitative Comparison of Binary Mix of Agro-Industrial Pozzolanic Additions for Elaborating Ternary Cements: Kinetic Parameters. *Materials* **2021**, *14*, 2944. [CrossRef] [PubMed]

13. Association Francaise de Génie Civil. *Ultra High Performance Fibre-Reinforced Concretes—Interim Recommendations*; AFGC: Paris, France, 2002. [CrossRef]
14. Zhang, Y.; Wang, S.; Yan, L. Transverse compressive characteristics of fiber reinforced cementitious composites tubes. *Thin-Walled Struct.* **2020**, *150*, 106645. [CrossRef]
15. Said, A.; Elsayed, M.; El-Azim, A.A.; Althoey, F.; Tayeh, B.A. Using ultra-high performance fiber reinforced concrete in improvement shear strength of reinforced concrete beams. *Case Stud. Constr. Mater.* **2022**, *16*, e01009. [CrossRef]
16. Smarzewski, P.; Barnat-Hunek, D. Effect of Fiber Hybridization on Durability Related Properties of Ultra-High Performance Concrete. *Int. J. Concr. Struct. Mater.* **2017**, *11*, 315–325. [CrossRef]
17. Abd El Hafez, R.D.; Ahmad, A.R.M.; Khafaga, M.A.; Al Zahraa Refaie, F. Effect of exposure to elevated temperatures on geopolymer concrete properties. *Int. J. Civ. Eng. Technol.* **2019**, *10*, 448–461.
18. Elsayed, M.; Tayeh, B.A.; Elmaaty, M.A.; Aldahshoory, Y. Behaviour of RC columns strengthened with Ultra-High Performance Fiber Reinforced concrete (UHPFRC) under eccentric loading. *J. Build. Eng.* **2022**, *47*, 103857. [CrossRef]
19. Li, Y.; Yang, E.-H.; Tan, K.H. Flexural behavior of ultra-high performance hybrid fiber reinforced concrete at the ambient and elevated temperature. *Constr. Build. Mater.* **2020**, *250*, 118487. [CrossRef]
20. Park, O.; Haftka, R.T.; Sankar, B.; Starnes, J.H.; Nagendra, S. Analytical-Experimental Correlation for a Stiffened Composite Panel Loaded in Axial Compression. *J. Aircr.* **2001**, *38*, 379–387. [CrossRef]
21. Buchanan, A.H.; Abu, A.K. *Structural Design for Fire Safety*; Wiley: New York, NY, USA, 2001; 421p.
22. Marvila, M.; de Azevedo, A.; de Matos, P.; Monteiro, S.; Vieira, C. Materials for Production of High and Ultra-High Performance Concrete: Review and Perspective of Possible Novel Materials. *Materials* **2021**, *14*, 4304. [CrossRef]
23. Kodur, V.; Raut, N. Performance of concrete structures under fire hazard: Emerging trends. *Indian Concr. J.* **2010**, *84*, 23–31.
24. Prem, P.R.; Bharatkumar, B.H.; Iyer, N.R. Influence of curing regimes on compressive strength of ultra high performance concrete. *Sadhana* **2013**, *38*, 1421–1431. [CrossRef]
25. Bautista-Toledo, M.; Méndez-Díaz, J.; Sanchez-Polo, M.; Rivera-Utrilla, J.; Ferro-García, M. Adsorption of sodium dodecylbenzenesulfonate on activated carbons: Effects of solution chemistry and presence of bacteria. *J. Colloid Interface Sci.* **2008**, *317*, 11–17. [CrossRef] [PubMed]
26. Dwaikat, M.; Kodur, V. Hydrothermal model for predicting fire-induced spalling in concrete structural systems. *Fire Saf. J.* **2009**, *44*, 425–434. [CrossRef]
27. Kodur, V.K.R.; Phan, L. Critical factors governing the fire performance of high strength concrete systems. *Fire Saf. J.* **2007**, *42*, 482–488. [CrossRef]
28. Tayeh, B.A.; Aadi, A.S.; Hilal, N.N.; Abu Bakar, B.H.; Al-Tayeb, M.M.; Mansour, W.N. Properties of ultra-high-performance fiber-reinforced concrete (UHPFRC)—A review paper. *AIP Conf. Proc.* **2019**, *2157*, 020040. [CrossRef]
29. Yu, X.M.; Zha, X.X.; Huang, Z.H. The Influence of Spalling on the Fire Resistance of RC Structures. *Adv. Mater. Res.* **2011**, *255–260*, 519–523. [CrossRef]
30. Banerji, S.; Kodur, V. Effect of temperature on mechanical properties of ultra-high performance concrete. *Fire Mater.* **2021**, *46*, 287–301. [CrossRef]
31. Palomo, A.; Grutzeck, M.W.; Blanco, M. Alkali-activated fly ashes-A cement for the future. *Cem. Concr. Res.* **1999**, *29*, 1323–1329. [CrossRef]
32. Thanon Dawood, E.; Abdullah, M.; Ismael, N.K. Effects Superplasticizer Type and Dosage on The Properties of Reactive Powder Concrete. *J. Civ. Eng. Inter Discip.* **2020**, *1*, 41–45. [CrossRef]
33. Abdelalim, A.; Bahaa, T.; Halawa, W.; El Hariri, M.O.R. Performance of reactive powder concrete produced using local materials. *HBRC J.* **2008**, *4*, 66–78.
34. Hassan, W.N.F.W.; Ismail, M.A.; Lee, H.-S.; Meddah, M.S.; Singh, J.K.; Hussin, M.W.; Ismail, M. Mixture optimization of high-strength blended concrete using central composite design. *Constr. Build. Mater.* **2020**, *243*, 118251. [CrossRef]
35. *ASTM C-597*; Standard Test Method for Pulse Velocity through Concrete. American Society for Testing and Materials: West Conshohocken, PA, USA, 2009.
36. *ASTM C1114-06*; Standard Test Method for Steady-State Thermal Transmission Properties by Means of the Thin-Heater Apparatus. ASTM International: West Conshohocken, PA, USA, 2006.
37. *British Standard 1881*; Testing Concrete. Part 207. Recommendations for the Assessment of Concrete Strength by Near-to-Surface Tests. British Standards Institute: London, UK, 1992.
38. *ASTM C293/C293M-16*; Standard Test Method for Flexural Strength of Concrete (Using Simple Beam with Center-Point Loading). ASTM International: West Conshohocken, PA, USA, 2010.
39. *ASTM C192/C192M-15*; Standard Practice for Making and Curing Concrete Test Specimens in the Laboratory. ASTM International: West Conshohocken, PA, USA, 2004.
40. *ASTM C469/C469M-14*; Standard Test Method for Static Modulus of Elasticity and Poisson's Ratio of Concrete in Compression. ASTM International: West Conshohocken, PA, USA, 2002.
41. Naaman, A.; Fischer, G.; Krustulovic-Opara, N. Measurement of tensile properties of fiber reinforced concrete: Draft submitted to ACI Committee 544. In Proceedings of the Rilem International Workshop on High Performance Fiber Reinforced Cement Composites (HPFRCC5), Mainz, Germany, 10–13 July 2007.

42. Cai, R.; Ye, H. Clinkerless ultra-high strength concrete based on alkali-activated slag at high temperatures. *Cem. Concr. Res.* **2021**, *145*, 106465. [CrossRef]
43. Sohail, M.G.; Wang, B.; Jain, A.; Kahraman, R.; Ozerkan, N.G.; Gencturk, B.; Dawood, M.; Belarbi, A. Advancements in Concrete Mix Designs: High-Performance and Ultrahigh-Performance Concretes from 1970 to 2016. *J. Mater. Civ. Eng.* **2018**, *30*, 04017310. [CrossRef]
44. Nematzadeh, M.; Tayebi, M.; Samadvand, H. Prediction of ultrasonic pulse velocity in steel fiber-reinforced concrete containing nylon granule and natural zeolite after exposure to elevated temperatures. *Constr. Build. Mater.* **2020**, *273*, 121958. [CrossRef]
45. Ramli, M.B.; Alonge, O.R. Characterization of metakaolin and study on early age mechanical strength of hybrid cementitious composites. *Constr. Build. Mater.* **2016**, *121*, 599–611. [CrossRef]
46. Nematzadeh, M.; Fallah-Valukolaee, S. Erosion resistance of high-strength concrete containing forta-ferro fibers against sulfuric acid attack with an optimum design. *Constr. Build. Mater.* **2017**, *154*, 675–686. [CrossRef]
47. Karimipour, A.; de Brito, J.; Edalati, M. Influence of polypropylene fibres on the thermal and acoustic behaviour of untreated coal coarse aggregates concrete. *J. Build. Eng.* **2021**, *36*, 102125. [CrossRef]
48. Algourdin, N.; Pliya, P.; Beaucour, A.-L.; Simon, A.; Noumowé, A. Influence of polypropylene and steel fibres on thermal spalling and physical-mechanical properties of concrete under different heating rates. *Constr. Build. Mater.* **2020**, *259*, 119690. [CrossRef]
49. Pehlivanlı, Z.O.; Uzun, I.; Yücel, Z.P.; Demir, I. The effect of different fiber reinforcement on the thermal and mechanical properties of autoclaved aerated concrete. *Constr. Build. Mater.* **2016**, *112*, 325–330. [CrossRef]
50. Wang, W.-C.; Wang, H.-Y.; Chang, K.-H.; Wang, S.-Y. Effect of high temperature on the strength and thermal conductivity of glass fiber concrete. *Constr. Build. Mater.* **2020**, *245*, 118387. [CrossRef]
51. Heniegal, A.M.; El-Habiby, F.F.; Hafez, R.D.A. Physical and mechanical properties of concrete incorporating industrial and agricultural textile wastes. *Int. J. Res. Eng. Technol.* **2015**, *4*, 166–176. [CrossRef]
52. Shen, P.; Zheng, H.; Liu, S.; Lu, J.-X.; Poon, C.S. Development of high-strength pervious concrete incorporated with high percentages of waste glass. *Cem. Concr. Compos.* **2020**, *114*, 103790. [CrossRef]
53. Li, T.; Huang, F.; Zhu, J.; Tang, J.; Liu, J. Effect of foaming gas and cement type on the thermal conductivity of foamed concrete. *Constr. Build. Mater.* **2019**, *231*, 117197. [CrossRef]
54. Sanjayan, G.; Stocks, L. Spalling of high-strength silica fume concrete in fire. *Mater. J.* **1993**, *90*, 170–173. [CrossRef]
55. Doherty, P.; Ali, F.; Nadjai, A.; Choi, S. Explosive Spalling of Concrete Columns with Steel and Polypropylene Fibres Subjected To Severe Fire. *J. Struct. Fire Eng.* **2012**, *3*, 95–104. [CrossRef]
56. Umasabor, R.; Okovido, J. Fire resistance evaluation of rice husk ash concrete. *Heliyon* **2018**, *4*, e01035. [CrossRef]
57. Madhavan, M.K.; Sathyan, D.; Jayanarayanan, K. Hybrid natural fiber composites in civil engineering applications. In *Hybrid Natural Fiber Composites*; Elsevier: Amsterdam, The Netherlands, 2021; pp. 41–72. [CrossRef]
58. Aslani, F.; Kelin, J. Assessment and development of high-performance fibre-reinforced lightweight self-compacting concrete including recycled crumb rubber aggregates exposed to elevated temperatures. *J. Clean. Prod.* **2018**, *200*, 1009–1025. [CrossRef]
59. Wu, H.; Lin, X.; Zhou, A. A review of mechanical properties of fibre reinforced concrete at elevated temperatures. *Cem. Concr. Res.* **2020**, *135*, 106117. [CrossRef]
60. Xiao, J.; Han, N.; Zhang, L.; Zou, S. Mechanical and microstructural evolution of 3D printed concrete with polyethylene fiber and recycled sand at elevated temperatures. *Constr. Build. Mater.* **2021**, *293*, 123524. [CrossRef]
61. Faried, A.S.; Mostafa, S.A.; Tayeh, B.A.; Tawfik, T.A. The effect of using nano rice husk ash of different burning degrees on ultrahigh-performance concrete properties. *Constr. Build. Mater.* **2021**, *290*, 123279. [CrossRef]
62. Heniegal, A.M. Performance of Concrete Incorporating Industrial and Agricultural Wastes. *IOSR J. Eng.* **2014**, *4*, 1–11. [CrossRef]
63. Selim, F.; Amin, M.S.; Ramadan, M.; Hazem, M.M. Effect of elevated temperature and cooling regimes on the compressive strength, microstructure and radiation attenuation of fly ash–cement composites modified with miscellaneous nanoparticles. *Constr. Build. Mater.* **2020**, *258*, 119648. [CrossRef]
64. Mastali, M.; Dalvand, A.; Sattarifard, A. The impact resistance and mechanical properties of the reinforced self-compacting concrete incorporating recycled CFRP fiber with different lengths and dosages. *Compos. Part B Eng.* **2017**, *112*, 74–92. [CrossRef]
65. Nili, M.; Afroughsabet, V. Combined effect of silica fume and steel fibers on the impact resistance and mechanical properties of concrete. *Int. J. Impact Eng.* **2010**, *37*, 879–886. [CrossRef]
66. Mezzal, S.K.; Al-Azzawi, Z.; Najim, K.B. Effect of discarded steel fibers on impact resistance, flexural toughness and fracture energy of high-strength self-compacting concrete exposed to elevated temperatures. *Fire Saf. J.* **2021**, *121*, 103271. [CrossRef]
67. Siemon, M.; Zehfuß, J. Experimental and numerical analysis of ultra high performance concrete (uhpc) members in case of fire. *Appl. Struct. Fire Eng.* **2016**, *125*, 103399. [CrossRef]
68. Xu, Z.; Li, J.; Wu, P.; Wu, C. Experimental investigation of triaxial strength of ultra-high performance concrete after exposure to elevated temperature. *Constr. Build. Mater.* **2021**, *295*, 123689. [CrossRef]

69. Sainz-Aja, J.A.; Gonzalez, L.; Thomas, C.; Rico, J.; Polanco, J.A.; Carrascal, I.; Setién, J. Effect of Steel Fibre Reinforcement on Flexural Fatigue Behaviour of Notched Structural Concrete. *Materials* **2021**, *14*, 5854. [CrossRef]
70. Chun, B.; Kim, S.; Yoo, D.-Y. Benefits of chemically treated steel fibers on enhancing the interfacial bond strength from ultrahigh-performance concrete. *Constr. Build. Mater.* **2021**, *294*, 123519. [CrossRef]